

The Brain Network Underlying the Recognition of Hand Gestures in the Blind: The Supramodal Role of the Extrastriate Body Area

Ryo Kitada,^{1,2} Kazufumi Yoshihara,³ Akihiro T. Sasaki,^{4,5} Maho Hashiguchi,^{1,2} Takanori Kochiyama,⁶ and Norihiro Sadato^{1,2,7}

¹Division of Cerebral Integration, National Institute for Physiological Sciences, Okazaki, 444–8585, Japan, ²Graduate University for Advanced Studies, Hayama, 240-0193, Japan, ³Department of Psychosomatic Medicine, Graduate School of Medical Sciences, Kyushu University, Fukuoka 812-8582, Japan, ⁴Department of Physiology, Osaka City University Graduate School of Medicine, Osaka, Japan, ⁵Pathophysiological and Health Science Team, RIKEN Center for Life Science Technologies, Kobe, 650-0047, Japan, ⁶ATR Brain Activity Imaging Center, Seika-cho 619-0288, Japan, and ⁷Biomedical Imaging Research Center, University of Fukui, Eiheiji, 910-1193, Japan

The visual perception of others' body parts is critical for understanding and imitating their behavior. The visual cortex in humans includes the extrastriate body area (EBA), which is a large portion of the occipitotemporal cortex that is selectively responsive to visually perceived body parts. Previous neuroimaging studies showed that the EBA not only receives sensory inputs regarding others' body information but also receives kinesthetic feedback regarding one's own actions. This finding raised the possibility that the EBA could be formed via nonvisual sensory modalities. However, the effect of visual deprivation on the formation of the EBA has remained largely unknown. Here, we used fMRI to investigate the effect of vision loss on the development of the EBA. Blind and sighted human subjects performed equally well in a haptic-identification task involving three categories of objects (hand shapes, toy cars, and teapots). The superior part (i.e., the middle temporal gyrus and angular gyrus) of the EBA and the supramarginal gyrus showed greater sensitivity to recognized hand shapes than to inanimate objects, regardless of the sensory modality and visual experience. Unlike the superior part of the EBA, the sensitivity of the inferior part (i.e., the inferior temporal sulcus and middle occipital gyrus) depended on visual experience. However, this vision-dependent sensitivity explained minor individual differences in hand-recognition performance. These results indicate that nonvisual modalities drive the development of the cortical network underlying the recognition of hand gestures with a node in the visual cortex.

Key words: EBA; fMRI; haptics; touch

Introduction

The visual perception of faces and body parts provides a wealth of information that is used to understand and imitate others' behaviors. Given its fundamental importance in the course of evolution, the innate neural mechanisms can anticipate the computations necessary for representing bodies. However, it

remains unclear how innate factors and postnatal experience interact to produce these underlying mechanisms.

One of the important nodes in the neural network underlying body perception resides in the lateral occipitotemporal cortex. Previous neuroimaging studies have identified a region called the extrastriate body area (EBA) that is more sensitive to visually perceived body parts than to other object categories (Downing et al., 2001). Recently, neuroimaging studies in sighted individuals have demonstrated that the EBA is more responsive to haptically recognized body parts than to inanimate objects (Kitada et al., 2009; Costantini et al., 2011). This finding raises the possibility that the EBA is involved in the supramodal representation of human bodies. A question that naturally follows is as follows: does the EBA develop without visual experience?

Although the EBA resides in the occipitotemporal cortex, previous fMRI studies provided surprising evidence that this region is also active when individuals execute self-actions (Astafiev et al., 2004; Orlov et al., 2010). This finding suggests that the EBA not only receives sensory inputs regarding others' body information, but also receives kinesthetic feedback regarding one's own actions. If the EBA receives kinesthetic information about self-

Received Feb. 4, 2014; revised June 18, 2014; accepted June 22, 2014.

Author contributions: R.K. designed research; R.K., K.Y., A.T.S., and M.H. performed research; T.K. contributed unpublished reagents/analytic tools; R.K. and T.K. analyzed data; R.K. and N.S. wrote the paper.

This work was supported by the Japan Society for the Promotion of Science Grant-in-Aid for Young Scientists (B) (25871059) and the Ministry of Education, Culture, Sports, Science and Technology of Japan Grant-in-Aid for Scientific Research on Innovative Areas, "Face perception and recognition" (23119727) to R.K., Ministry of Education, Culture, Sports, Science and Technology of Japan Grant-in-Aid for Scientific Research S (21220005) and "Development of biomarker candidates for social behavior" performed under the Strategic Research Program for Brain Sciences to N.S., and the Canadian Institutes of Health Research and the Natural Sciences and Engineering Research Council of Canada to S. J. Lederman at Queen's University. We thank Y. Miyawaki for valuable comments on the earlier manuscript.

The authors declare no competing financial interests.

Correspondence should be addressed to Dr. Ryo Kitada, Division of Cerebral Integration, National Institute for Physiological Sciences, Okazaki, 444-8585, Japan. E-mail: kitada@nips.ac.jp.

DOI:10.1523/JNEUROSCI.0500-14.2014

Copyright © 2014 the authors 0270-6474/14/3410096-13\$15.00/0

Table 1. Blind subjects

Subject	Sex	Age (years)	Onset of total blindness (years)	Cause of total blindness	Residual vision
B01	M	33	0	Retinopathy of prematurity	Light perception
B02	M	35	3	Glaucoma	No
B03	M	41	13	Retinal detachment	No
B04	M	39	0	Retinopathy of prematurity	No
B05	F	52	0	Chorioretinal atrophy	Light perception
B06	M	22	0	Congenital cataract	No
B07	M	22	0	Retinoblastoma	No
B08	F	25	0	Retinopathy of prematurity	Light perception
B09	M	22	2	Retinoblastoma	No
B10	M	26	15	Congenital cataract	No
B11	M	37	10	Retinal detachment	Light perception
B12	M	38	2	Cancer	No
B13	M	61	20	Retinitis pigmentosa	No
B14	M	25	9	Glaucoma	No
B15	M	40	0	Retinopathy of prematurity	No
B16	M	31	0	Microphthalmia	No
B17	M	23	0	Retinopathy of prematurity	No
B18	M	28	0	Retinopathy of prematurity	No
B19	F	25	0	Retinopathy of prematurity	No
B20	F	26	0	Retinopathy of prematurity	Light perception
B21	M	26	0	Amaurosis	Light perception
B22	F	24	0	Congenital rubella syndrome	No
B23	M	37	0	Microphthalmus	No
B24	F	26	0	Retinopathy of prematurity	Light perception
B25	F	27	2	Keratomalacia	Light perception
B26	F	47	0	Congenital unknown disease	Light perception
B27	F	64	7	Congenital cataract	No
B28	M	31	0	Retinoblastoma	No

actions, it might be expected to develop body selectivity even in the absence of vision.

Recent neuroimaging studies involving congenitally blind individuals have shown that category sensitivity develops without visual experience in several regions within the ventral visual pathway (Reich et al., 2011; Wolbers et al., 2011; Striem-Amit et al., 2012; He et al., 2013; Peelen et al., 2013). However, to the best of our knowledge, only one previous study has tested the effect of visual deprivation on the development of the EBA. Striem-Amit and Amedi (2014) demonstrated that the EBA in congenitally blind individuals is sensitive to full-body shapes conveyed through a sensory-substitution device after prolonged, intensive training. However, the sensory-substitution device is not necessary for perceiving body parts; blind individuals can recognize body parts and learn their actions via haptics during daily life. If the EBA is essential for body perception in the absence of vision, this region should show sensitivity to body parts when a blind individual recognizes them in an ecologically valid manner.

Here we used fMRI to examine the effect of visual experience on the functional specialization of the EBA in sighted and blind participants. We used a haptic object-identification task to examine the degree of body sensitivity in the EBA (Kitada et al., 2009). We predicted that the EBA develops its body preference regardless of visual experience.

Materials and Methods

Subjects

A total of 28 blind (19 males and 9 females, mean age ± SD, 33.5 ± 11.1 years) and 28 sighted (19 males and 9 females, mean age ± SD = 33.3 ± 11.4 years) individuals participated in the study (Table 1). Eighteen of the subjects in the blind group reported having experienced total loss of sight

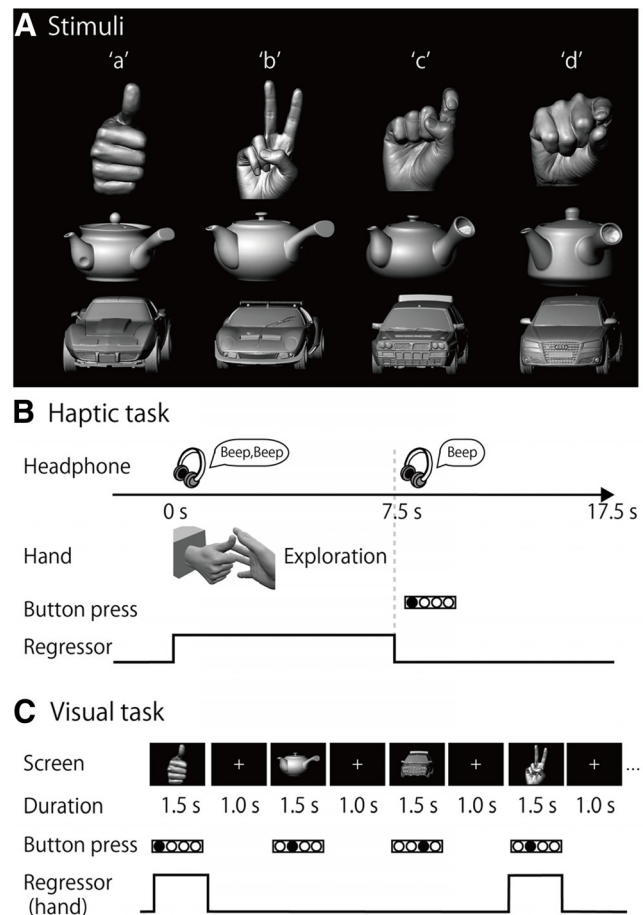


Figure 1. Task. **A**, Stimuli. Plastic casts of hands, teapots, and toy cars were used as stimuli. An alphabetic code (a–d) was assigned to the four exemplars of each object category. **B**, Haptic task. Subjects were instructed to explore the object with their right hand immediately after they heard a sound cue through headphones. When a second sound cue was presented (after 7.5 s of exploration), the subjects were told to stop. They were instructed to respond by using their left hand to press the button corresponding to the appropriate alphabetic code. **C**, Visual task. Sighted subjects were instructed to identify the four exemplars of each object category by pressing the same buttons as used in the haptic task. For both haptic and visual tasks, neural activity during the task block was modeled with a boxcar function for each object category. The regressor shown was convolved with a canonical hemodynamic response function.

within 12 months of birth and were categorized as congenitally blind; the remainder were defined as noncongenitally blind. There was no significant difference in age between the groups (*t* test, *p* = 0.96). All subjects were right-handed (Oldfield, 1971). None of the subjects reported a history of major medical or neurological illness, such as epilepsy, significant head trauma, or a lifetime history of alcohol dependence. All of the subjects gave written informed consent for participation in the study. The protocol was approved by the local medical ethics committee at the National Institute for Physiological Sciences (Aichi, Japan).

Stimuli

The three classes of objects used were plastic casts of hands, toy cars, and teapots (Fig. 1A). Toy cars and teapots were included as nonbiological control objects because they are common, complex 3D objects, which have many exemplars and are similar in size to hands. Four exemplars were prepared for each class (4 exemplars × 3 classes = 12 objects in total; Fig. 1A). An actor made four different hand shapes for the hand exemplars. The actor’s hand, the toy cars, and the teapots were scanned with a 3D digitizer (MH, Artec Group for the hand stimuli; ATOS, GOM for the objects) and plastic casts were created using a 3D printer (Connex 500, Stratasys).

Data acquisition

fMRI was performed using a 3T Siemens Allegra whole-head system (Siemens). Standard sequence parameters were used to obtain gradient-echo echo-planar images (EPIs) as follows: repetition time (TR) = 2500 ms; echo time (TE) = 30 ms; flip angle = 80°; 39 3 mm axial slices with a 17% slice gap; field of view = 192 × 192 mm; and in-plane resolution = 3.0 × 3.0 mm. A T1-weighted high-resolution anatomical image was obtained from each participant (voxel size = 0.9 × 0.9 × 1 mm) between the functional imaging runs.

Haptic-identification task

Stimulus presentation. The procedure used was as described previously (Kitada et al., 2010, 2013). The subjects lay supine on the scanner bed with their eyes closed, wearing MRI-compatible headphones (Kiyohara Optics), and were instructed to relax. The right hand was used to explore the stimuli, while the left arm was extended along the side of the subject's body and the left hand held a response pad. Each subject completed six runs of the task (99 volumes per run, 247.5 s). A single run consisted of a 27.5 s rest period, followed by a 210 s task period, and a 10 s rest period. Each of the 12 exemplars was presented once during the task period, for 7.5 s (Fig. 1B). This trial duration was chosen based on results from our previous study (Kitada et al., 2013), in which 7.5 s was sufficient for the subjects to identify familiar objects after a short period of training. The presentation of objects alternated with 10.0 s interstimulus intervals (ISIs), during which subjects identified the previous object with a key press (17.5 s × 12 exemplars = 210 s in total). The order in which the objects were presented in a single run was pseudo-randomized using a genetic algorithm that maximized the estimation efficiency for the tested contrasts (Wager and Nichols, 2003). Presentation software (Neurobehavioral Systems) was used to present auditory cues to the subjects via headphones and visual cues to the experimenter during the haptic-identification task. Presentation software was also used to present the stimuli (hands, toy cars, and teapots) during the subsequent visual-identification task.

Task

Before the fMRI experiment, subjects were blindfolded and trained to identify the stimulus objects until they felt comfortable performing the task. Training with corrective feedback was necessary to minimize activation due to possible differences in task difficulty between the identification of hands and inanimate objects. During training, subjects were asked to identify exemplars for each object class. Training took <30 min.

In each trial, subjects were instructed to start exploring the object as soon as they heard a brief sound cue (Fig. 1B). Another cue was presented 7.5 s after the trial was initiated. Subjects were asked to identify the exemplar immediately by pressing one of four buttons. To match the sensorimotor requirements between object classes, subjects were instructed to continue exploring the object to confirm their answer, even if they had identified it within 7.5 s. The experimenter (R.K.) visually confirmed that the hand movements used to explore the objects were comparable across the object categories in terms of exploratory procedures (enclosure and contour following) (Lederman and Klatzky, 1987).

Visual-identification task

After completion of the haptic task, sighted subjects participated in a visual-identification task to enable us to examine the brain regions involved in the visual identification of hand shapes.

Stimulus presentation

Two monochromatic images of each exemplar were used for the task (2 images × 12 exemplars = 24 images in total; Fig. 1A). The differences in size and perceived brightness of these images were minimized using photo-editing software (Photoshop, Adobe Systems). The subjects fixated on a white cross on the screen, which they viewed through a mirror attached to the head coil. Stimuli were back-projected via a liquid crystal display projector (LT 265, NEC Viewtechnology) onto a translucent screen located at the rear of the scanner. The stimuli and the white fixation cross subtended visual angles of ~7.8° and 0.8°, respectively. During the visual task, the right hand did not touch any object, and the left hand held the response pad.

Task

Similar to the haptic task, the visual-identification task required the subjects to identify the stimuli presented in a pseudo-randomized order. The visual-identification task consisted of six runs (115 volumes per run, 287.5 s), and a single run consisted of a 240 s task period that was preceded by a 27.5 s fixation (rest) period and followed by a 20 s fixation (rest) period. During the task period, each image was presented three times. Each image appeared for 1.5 s with an ISI of 1.0 s (2.5 s × 3 times × 2 images × 4 exemplars × 3 object classes = 180 s; Fig. 1C). In addition, we inserted null trials, which were identical to the trials, except that no picture was presented (2.5 s × 24 trials = 60 s). The order of stimulus presentation and null trials within a single run was pseudo-randomized using the algorithm used in the haptic-identification task. Subjects were asked to identify the exemplars of each object class by pressing one of four buttons. The fMRI experiment was conducted after ~10 min of training.

EBA localizer task

A conventional block design was used to localize the EBA (Downing et al., 2001; Peelen and Downing, 2005a,b). Each sighted subject was asked to observe monochromatic images of body parts, faces, teapots, and cars. The images were different from those used in the visual-identification task. Each run consisted of 21 blocks that lasted for 15 s. The 1st, 6th, 11th, 16th, and 21st blocks were fixation-only baseline conditions. Twenty photographs from one of the four object categories were presented successively in each block. Each photograph was presented for 300 ms, and the ISI was 450 ms. Each object category block was repeated four times (5 baseline blocks + 4 object categories × 4 repetitions = 21 blocks; 15 s × 21 blocks = 315 s; 126 volumes in total). A 12.5 s fixation-only baseline condition was added before the first baseline block (126 + 5 = 131 volumes). A fixation cross changed its color from white to red twice during the ISIs in each block. Sighted subjects were asked to press a button with their right hand as soon as the fixation cross turned red. Each sighted subject completed two runs of the localizer task.

Data processing

Image processing and statistical analyses were performed using the Statistical Parametric Mapping (SPM8) package (Friston et al., 2007) (RRID: nif-0000-00343). The first five volumes of each fMRI run were discarded to allow the MR signal to reach a state of equilibrium. The remaining volumes were used for the subsequent analyses. To correct for subject's head motion, functional images from each run were realigned to the first image, and again realigned to the mean image after the first realignment. Slice-timing correction was then performed to adjust for differences in slice-acquisition times. The T1-weighted anatomical image was coregistered to the mean of all realigned images. Before coregistration, the T1-weighted anatomical image was skull stripped to prevent the nonbrain tissue from affecting the alignment between the EPI and T1 images. Each coregistered T1-weighted anatomical image was normalized to the MNI space with the DARTEL procedure (Ashburner, 2007). More specifically, each anatomical image was segmented into the tissue class images using a unified segmentation approach (Ashburner and Friston, 2005). The gray and white matter images were transformed to a common coordinate space to create a study-specific template using the DARTEL registration algorithm. The study-specific template was then affine normalized to MNI space with the ICBM Probabilistic Atlases (http://www.bmap.ucla.edu/portfolio/atlas/ICBM_Probabilistic_Atlases/). The parameters from the DARTEL registration and normalization to MNI space were then applied to each functional image and the T1-weighted anatomical image. The normalized functional images were filtered using a Gaussian kernel of 4 mm FWHM in the *x*, *y*, and *z* axes.

Statistical analysis

Linear contrasts between conditions in the haptic and visual tasks were calculated for individual subjects, and incorporated into a random-effects model to make inferences at a population level (Holmes and Friston, 1998).

Initial individual analysis

A GLM was fitted to the fMRI data for each subject (Friston et al., 1994; Worsley and Friston, 1995). The BOLD signal for all the tasks was mod-

Behavioral Performance

Haptics

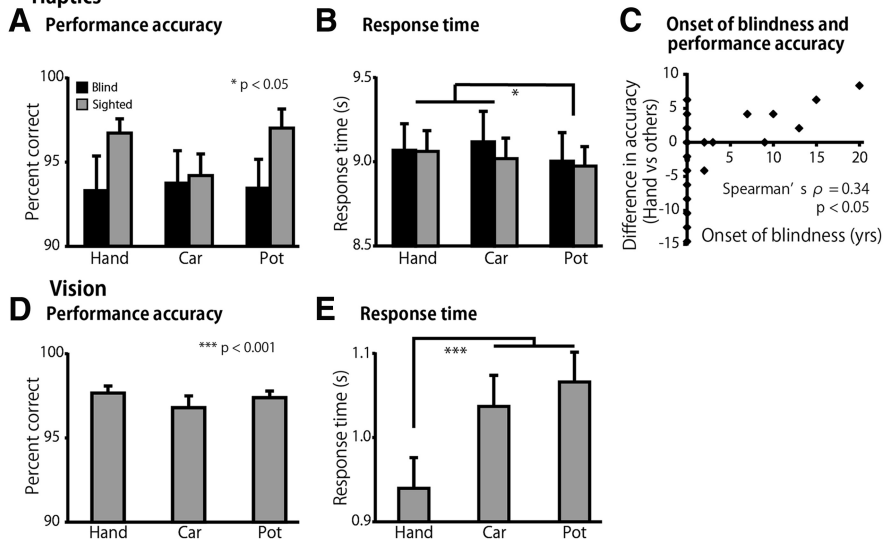


Figure 2. Behavioral performance. Performance accuracy and response time for the haptic task (**A**, **B**) and for the visual task (**D**, **E**). Asterisks indicate the results of *post hoc* pairwise comparisons between object categories (with a Sidak–Bonferroni correction). **C**, Difference in accuracy indicates the relative performance accuracy for hand recognition (calculated as performance accuracy for the hand recognition – performance accuracy for the other two object categories). We found a significant correlation between the age at onset of total blindness and the relative performance accuracy scores (Spearman's $\rho = 0.34$, $p < 0.05$). Data are presented as the mean \pm SEM of 28 blind and 28 sighted subjects.

eled with boxcar functions convolved with the canonical hemodynamic response function. For each subject in each group, a design matrix comprising the six runs of the haptic-identification task was prepared. Each run in the haptic task included three task-related regressors, one for each object category. Another design matrix, which included the six runs of the visual-identification task, was prepared for the sighted subjects. Each run in the visual task included four task-related regressors, one for each object category and the other for null trials. Finally, we prepared a design matrix including the two runs of the EBA localizer task. The time series for each voxel was high-pass filtered at 1/128 Hz. Assuming a first-order autoregressive model, the serial autocorrelation was estimated from the pooled active voxels with the restricted maximum likelihood procedure and was used to whiten the data (Friston et al., 2002). Motion-related artifacts were minimized by incorporating the six parameters (three displacements and three rotations) from the rigid-body realignment stage into each model. Three additional regressors, describing intensities in white matter, CSF, and residual compartments (outside the brain and skull), were added to the model to account for image-intensity shifts attributable to the movement of the hand within the main magnetic field of the scanner (Grol et al., 2007; Kitada et al., 2013). The estimates for each object category were evaluated using linear contrasts.

Subsequent random-effects group analysis

Contrast images from the individual analyses were used for the group analysis, with between-subjects variance modeled as a random factor. The contrast images obtained from the individual analyses represent the normalized task-related increment of the MR signal of each subject. We produced three design matrices: one for the EBA localizer task, one for the identification tasks for both blind and sighted subjects, and one for the analysis of the effect of the onset of total blindness on hand sensitivity. In all design matrices, the estimates for the conditions were compared using linear contrasts. The resulting set of voxel values for each contrast constituted the SPM{t}, which was transformed into normal distribution units (SPM{z}). The threshold for the SPM{z} was set at $Z > 2.58$ (equivalent to $p < 0.005$ uncorrected). The statistical threshold for the spatial extent test on the clusters was set at $p < 0.05$ and corrected for multiple comparisons over the search volume (Friston et al., 1996). Brain regions were anatomically defined and labeled according to a probabilistic atlas (Shattuck et al., 2008) and an anatomical MRI averaged over all sub-

jects. The NeuroElf toolbox (version 0.9c; <http://neuroelf.net/>) and Brain Voyager QX (Brain Innovation) were used to display activation patterns on a surface-rendered T1-weighted MRI averaged across the subjects.

EBA localizer task. A full factorial design was used to construct a single design matrix, including the four different categories. As in previous studies (Peelen and Downing, 2005a,b), the EBA was defined by comparing the observed body parts with the mean for the other three categories. The search volume was the whole brain.

Object-identification task. A flexible factorial design was used to construct a single design matrix involving the visual- and haptic-identification tasks in the sighted individuals and the haptic-identification tasks in the blind individuals. Conditions for sighted and blind individuals were modeled as separate between-subject (independent) levels, whereas conditions within each group were modeled as within-subject (dependent) levels. We evaluated the predefined contrasts described below. In the following analyses, we initially defined the search volume for activation as the whole brain (whole-brain analysis). Subsequently, the search volume was limited to the EBA in each hemisphere to examine the effects of visual deprivation on this region (i.e., ROI analysis).

The present study examined whether the formation of hand-sensitive activity in the EBA requires visual experience. Three possibilities were considered: (1) that visual experience is unnecessary; (2) that the length of visual experience is critical; and (3) that visual experience is necessary. The following analyses were conducted to examine these possibilities.

Brain regions showing hand sensitivity in both groups. Initially, the identification of hand shapes was compared with the mean identification of inanimate objects for each of the three conditions: the haptic condition in the sighted participants (*sighted Hh vs Hi*), the visual condition in the sighted participants (*sighted Vh vs Vi*), and the haptic condition for the blind participants (*blind Hh vs Hi*). The conjunction of *sighted Hh vs Hi*, *sighted Vh vs Vi*, and *blind Hh vs Hi* was then analyzed to depict the brain regions showing hand selectivity regardless of the sensory modality or visual experience (the conjunction-null hypothesis) (Friston et al., 2005; Nichols et al., 2005). This conjunction analysis included data from only the congenitally blind subjects.

Group differences. To examine the brain regions in which there was reduced hand sensitivity in the blind group, *sighted Hh vs Hi* was compared with *blind Hh vs Hi* within the brain regions activated by the conjunction of *sighted Hh vs Hi* and *sighted Vh vs Vi*. Likewise, the brain regions showing greater hand sensitivity in the blind group than in the sighted group were depicted by comparing *blind Hh vs Hi* with *sighted Hh vs Hi* within the brain regions activated by *blind Hh vs Hi*. The data from all of the blind subjects were included in these analyses.

Effect of age at onset of total blindness. Simple regression analysis was conducted to determine the brain regions in which the response during the hand-recognition task was correlated with the age at onset of total blindness. As the majority of the subjects were congenitally blind, the assumption of parametric tests might have been violated. Hence, the analysis was performed using nonparametric permutation tests with the Statistical nonParametric Mapping (SnPM13) toolbox (Nichols and Holmes, 2002) (RRID: nif-0000-00342).

Cross-validation analysis

Supplemental cross-validation analysis was used to determine whether a region within the EBA showed a greater response to the perceived hand than to each of the inanimate objects while avoiding the double-dipping problem (Kriegeskorte et al., 2009).

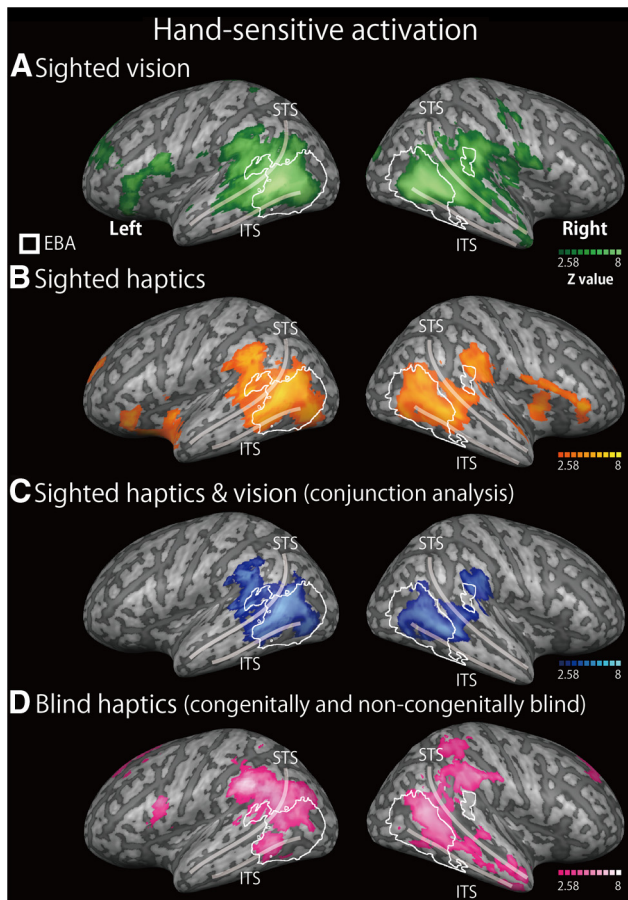


Figure 3. Hand-sensitive activation in sighted and blind individuals. We compared the activation during the recognition of hand stimuli with the mean activation during the recognition of other inanimate objects (the hand-sensitive activation) for three conditions: the visual task in the sighted group (A), the haptic task in the sighted group (B), and the haptic task in the blind group (both congenitally and noncongenitally) (D). The overlapping activation between the haptic and vision tasks in the sighted group (blue area) was evaluated statistically using a conjunction analysis (C). Regions within the white line indicate the EBA, which was defined by an independent visual-localizer task. The activation maps were thresholded at $p < 0.05$, corrected for multiple comparisons, with the height threshold set at $Z > 2.58$. The results were superimposed on a surface-rendered T1-weighted high-resolution MRI averaged across the subjects. STS, Superior temporal sulcus; ITS, inferior temporal sulcus. See Tables 3 and 4 for more details of peak coordinates.

Data from the haptic task of each subject were split into two independent sets (three odd runs and three even runs). A peak coordinate of activation evaluated by Hh vs Hi was localized in the odd runs, and contrast estimates were extracted from the same coordinate in the even runs. A peak coordinate within the EBA was sought in each hemisphere at the same height threshold as the random-effect analysis (Z value > 2.58). The procedure was repeated by defining a peak coordinate in the even runs and extracting contrast estimates in the odd runs. In the sighted subjects, contrast estimates of the visual task were also extracted from the coordinates identified by Hh vs Hi in each individual. The peak coordinates and contrast estimates obtained by the two procedures in each individual were averaged.

Results

Both the blind (18 congenitally blind and 10 noncongenitally blind) subjects and the sighted subjects completed the object-identification task. All subjects haptically identified hand shapes and 3D casts of the other object categories (i.e., teapots and toy cars). The sighted subjects also completed a visual-identification

Table 2. EBA^a

Spatial extent test/cluster size (mm ³)	p values	MNI coordinates			Z value	Hemisphere	Anatomical region
		x	y	z			
20672	<0.001	-48	-70	6	Inf	L	Middle occipital gyrus
		-48	-62	0	7.0	L	Middle temporal gyrus
		-64	-52	14	5.0	L	Superior temporal gyrus
		-52	-70	-20	3.6	L	Inferior occipital gyrus
		-38	-60	0	4.9	L	Fusiform gyrus
		-22	-84	36	6.2	L	Superior occipital gyrus
		-54	-60	12	7.5	L	Angular gyrus
20320	<0.001	52	-66	12	7.2	R	Middle occipital gyrus
		56	-60	0	Inf	R	Middle temporal gyrus
		66	-42	16	3.8	R	Superior temporal gyrus
		48	-56	-2	7.8	R	Inferior temporal gyrus
		42	-58	-4	3.6	R	Fusiform gyrus
		26	-82	36	5.9	R	Superior occipital gyrus
		46	-60	12	6.5	R	Angular gyrus
		62	-34	26	4.1	R	Supramarginal gyrus

^aThe activation was thresholded at $p < 0.05$, corrected for multiple comparisons over the whole brain, with the height threshold set at $Z > 2.58$. x , y , and z are stereotaxic coordinates (mm). Inf, Z value > 8.0 ; R, right; L, left.

task involving the 3D objects used in the haptic task, and a conventional EBA localizer task (Downing et al., 2001).

Task performance

Haptic object-identification task

The performance accuracy was $>90\%$ in all categories, regardless of the group (Fig. 2A). A two-way ANOVA (3 object categories \times 2 groups) using the accuracy scores showed neither a significant main effect nor an interaction (p values > 0.1). The response times were ~ 9.0 s from the onset of exploration in all the conditions (Fig. 2B). The same ANOVA performed on the response times revealed a significant main effect of object category ($F_{(2,108)} = 6.2$, $p < 0.01$). *Post hoc* pairwise comparisons (with a Sidak–Bonferroni correction) revealed significantly shorter response times for the teapot category than the hand and toy car categories (76 ms, p values < 0.05). There was neither a significant main effect of group nor an interaction with object category (p values > 0.1).

Age at onset of total blindness predicted performance accuracy in hand recognition

We examined to what extent the age at onset of total blindness predicted performance accuracy in the recognition of hand shapes. To exclude factors nonspecific to the recognition of hand shapes, the relative performance accuracy for hand recognition was calculated by subtracting the performance accuracy for inanimate objects from that for hand shapes. We found a significant correlation between the age at onset of total blindness and the relative performance accuracy scores (Spearman's $\rho = 0.34$, $p < 0.05$, Fig. 2C).

Visual object-identification task

The performance accuracy was comparable for all the categories (Fig. 2D). A one-way ANOVA (three categories) for accuracy scores produced no significant main effect ($p = 0.4$). The same ANOVA performed on response times revealed a significant main effect ($F_{(2,54)} = 45.7$, $p < 0.001$). *Post hoc* pairwise comparisons (with a Sidak–Bonferroni correction) revealed that the response times for the hand shapes were significantly shorter than those for toy cars and teapots (p values < 0.001 ; Fig. 2E).

Table 3. Hand-sensitive activation in the sighted and blind subjects^a

Spatial extent/test/cluster size (mm ³)	<i>p</i> values	MNI coordinates			<i>Z</i> value	Hemisphere	Anatomical region
		<i>x</i>	<i>y</i>	<i>z</i>			
Overlap of hand-sensitive activation between vision and haptics in the sighted (conjunction analysis, Fig. 3C)							
19104	<0.001	−42	−76	4	4.6	L	Middle occipital gyrus
		−58	−46	−2	5.3	L	Middle temporal gyrus
		−64	−46	8	5.5	L	Superior temporal gyrus
		−56	−40	30	5.1	L	Supramarginal gyrus
		−48	−58	16	5.6	L	Angular gyrus
8224	<0.001	−38	−70	−2	3.3	L	Inferior occipital gyrus
		48	−66	0	4.0	R	Middle occipital gyrus
		60	−50	4	5.0	R	Middle temporal gyrus
		48	−38	6	3.5	R	Superior temporal gyrus
		48	−60	24	3.4	R	Angular gyrus
2016	<0.001	58	−62	−4	3.5	R	Inferior temporal gyrus
		62	−30	28	4.4	R	Supramarginal gyrus
2256	<0.001	−4	54	8	4.0	L	Superior frontal gyrus
		4	52	16	4.1	R	Superior frontal gyrus
		0	42	4	3.0		Cingulate gyrus
Hand-sensitive activation in the blind (both congenital and noncongenital, Fig. 3D)							
21408	<0.001	−48	−78	24	5.2	L	Middle occipital gyrus
		−60	−56	0	5.2	L	Middle temporal gyrus
		−52	−56	−6	3.6	L	Inferior temporal gyrus
		−60	−50	20	4.1	L	Superior temporal gyrus
		−46	−74	32	5.0	L	Angular gyrus
15896	<0.001	−60	−38	38	6.8	L	Supramarginal gyrus
		54	−68	4	3.8	R	Middle occipital gyrus
		60	−56	8	4.5	R	Middle temporal gyrus
		58	−46	10	3.9	R	Superior temporal gyrus
		44	−52	14	5.8	R	Angular gyrus
4592	<0.001	58	−38	46	5.1	R	Supramarginal gyrus
		46	−42	58	4.4	R	Superior parietal lobule
		−8	−60	34	3.4	L	Precuneus
		−12	−54	40	4.2	L	Superior parietal lobule
		−8	−48	32	5.0	L	Cingulate gyrus
2064	<0.001	6	−42	26	4.7	R	Cingulate gyrus
		52	−12	−28	3.4	R	Inferior temporal gyrus
		48	−2	−30	3.8	R	Middle temporal gyrus
1480	<0.01	50	6	−24	4.2	R	Superior temporal gyrus
		48	−40	30	3.2	R	Angular gyrus
		44	−36	40	4.0	R	Supramarginal gyrus
1192	<0.05	34	−42	42	4.0	R	Superior parietal lobule
		24	40	34	3.2	R	Superior frontal gyrus
		8	46	38	4.9	R	Superior frontal gyrus
7336	<0.001	24	40	34	3.2	R	Middle frontal gyrus
		−12	40	−6	4.7	L	Superior frontal gyrus
		6	48	−2	4.1	R	Superior frontal gyrus
2472	<0.001	−2	40	0	4.1	L	Cingulate gyrus
		6	36	8	3.8	R	Cingulate gyrus
		−12	26	60	4.6	L	Superior frontal gyrus
1032	<0.05	−24	22	54	3.3	L	Middle frontal gyrus
		−46	6	18	4.3	L	Precuneus
		−50	12	10	4.2	L	Inferior frontal gyrus
1536	<0.01	22	−86	−42	5.1	R	Cerebellum
1360	<0.01	42	−60	−44	5.0	R	Cerebellum

^aThe activation was thresholded at $p < 0.05$, corrected for multiple comparisons over the whole brain, with the height threshold set at $Z > 2.58$. *x*, *y*, and *z* are stereotaxic coordinates (mm). R, Right; L, left.

fMRI results

To examine the effect of visual deprivation in detail at the group level, we normalized and smoothed the fMRI data using a sophisticated procedure with a 4 mm smoothing kernel (DARTEL) (Ashburner, 2007). The statistical threshold was set at $p < 0.05$, corrected at the cluster level when the *Z* value was > 2.58 (equivalent to $p < 0.005$ uncorrected).

EBA

The EBA was initially defined by comparing the brain response to visually observed body parts with the mean response to the other

categories (faces, cars, and teapots) in the EBA localizer task. This comparison revealed bilateral clusters of activation in the lateral occipitotemporal cortex (Fig. 3; Table 2). The EBA is a large region, extending over different gyri within the lateral occipitotemporal cortex (Spiridon et al., 2006; Weiner and Grill-Spector, 2011) and in the angular gyrus (Astafiev et al., 2004). Consistent with these previous findings, the clusters in both hemispheres included the middle occipital gyrus, middle temporal gyrus, fusiform gyrus, and angular gyrus. In addition to these regions, we found activation in the bilateral superior temporal gyrus, the bilateral superior occipital gyrus, left inferior occipital gyrus, right supra-

Table 4. Correspondence of hand-sensitive activation between the conditions^a

Anatomical location	Hemisphere	Vision (Fig. 3A) MNI coordinate				Sighted haptics (Fig. 3B) MNI coordinate				Distance (mm)	Blind haptics (all) (Fig. 3D) MNI coordinate				Distance (mm)
		x	y	z	Z value	x	y	z	Z value		x	y	z	Z value	
Middle occipital gyrus	L	−48	−68	8	7.8	−42	−78	2	5.2	13.1	−48	−78	24	5.2	18.9
	R	40	−60	4	Inf	−50	−70	10	4.2	3.5*	−48	−80	10	3.1	12.2
Middle temporal gyrus	L	−54	−62	10	Inf	50	−66	−2	4.1	13.1	48	−76	22	4.0	25.4
	R	50	−54	6	Inf	40	−52	4	3.4	8.0	54	−68	4	3.8	16.1
Superior temporal gyrus	L	−58	−58	12	Inf	−58	−46	0	5.6	19.3	−60	−56	0	5.2	13.1
	R	64	−42	10	5.8	−56	−62	8	4.6	2.8*	−50	−62	10	3.1	4.0*
Angular gyrus	L	−54	−62	12	Inf	60	−50	4	5.0	11.0	48	−56	12	5.5	6.6
	R	46	−58	12	6.1	48	−56	8	4.2	3.5*	−54	−4	−12	4.1	59.2
Supramarginal gyrus	L	−58	−40	30	6.1	−58	−58	16	4.5	4.0*	−62	−58	14	3.3	4.5*
	R	54	−28	24	5.5	54	−32	8	3.7	14.3	58	−46	10	3.9	7.2
Inferior occipital gyrus	L	−36	−68	0	5.1	66	−42	10	3.0	2.0*	64	−28	36	5.0	15.6
	R		NS			−38	−78	−6	4.2	11.8		NS			
Inferior temporal gyrus	L	−42	−64	0	3.8	−38	−70	−2	3.3	3.5*		NS			
	R	42	−58	2	7.6	46	−56	12	3.02	2.0*	−52	−56	−6	3.6	14.1
						58	−62	−4	3.5	17.5	52	−12	−28	3.4	55.8
						40	−54	2	3.0	4.5*					

^aWe localized peak coordinates of hand-sensitive region in each anatomically defined region (Shattuck et al., 2008) in each condition (vision, sighted haptics, and blind haptics). We also listed other coordinates at local maxima in each region, if these were more adjacent to the visually defined peak coordinate. R, Right; L, left.

*Distance from peak coordinates in the visual condition is <6.5 mm, the effective spatial resolution (final smoothness defined as FWHM). NS indicates that no peak coordinate was found.

marginal gyrus, and right inferior temporal gyrus. These two clusters of activation were defined as the EBA in this study.

Hand-sensitive activation

We evaluated the contrast of hand stimuli versus the mean of the other inanimate objects in each condition in the object-identification task, to identify hand-sensitive activation. Two analyses were conducted: whole-brain analysis, in which the search volume was the whole brain; and ROI analysis, in which the search volume was limited to the EBA in each hemisphere.

The sighted group

We initially depicted the hand-sensitive activation in each sensory modality in the sighted subjects. For both vision and touch, the whole-brain analysis showed regions of significant activation in the lateral occipitotemporal cortex bilaterally (Fig. 3A, B). We then conducted conjunction analysis to examine the overlap of the hand-sensitive activation between vision and touch. The whole-brain analysis revealed regions of significant activation in the occipitotemporal cortex: the bilateral middle occipital gyrus, bilateral middle temporal gyrus, bilateral superior temporal gyrus, left inferior occipital gyrus, and right inferior temporal gyrus (Fig. 3C; Table 3). Moreover, we also observed activation bilaterally in the angular gyrus, supramarginal gyrus, superior frontal gyrus, and cingulate gyrus. As shown in Figure 3, we confirmed that this activation showed substantial overlap with the EBA.

Table 4 indicates the correspondence of the peak coordinates of hand-sensitive activation between vision and touch in and around the lateral occipitotemporal cortex. The location of the highest peak coordinates for the visual and haptic conditions differed beyond the effective spatial resolution of 6.5 mm (de-

defined as the FWHM). However, the local peak coordinates (local maxima) of haptic activation were within 6.5 mm of the peak coordinates in the visual conditions in the following regions: the left middle occipital gyrus, bilateral middle temporal gyrus, bilateral superior temporal gyrus, right angular gyrus, bilateral supramarginal gyrus, left inferior occipital gyrus, and right inferior temporal gyrus (MNI coordinates indicated with asterisks in Table 4).

The blind group

Activation in the blind group was examined during haptic hand identification. Whole-brain analysis revealed regions of significant activation in the bilateral occipitotemporal cortex: the middle occipital gyrus, middle temporal gyrus, superior temporal gyrus, and inferior temporal gyrus. In addition, regions of significant activation were seen bilaterally in the angular gyrus, supramarginal gyrus, superior parietal lobule, cingulate gyrus, superior frontal gyrus, and middle frontal gyrus. Lateralized activation was observed in the left precuneus, left precentral gyrus, left inferior frontal gyrus, and right cerebellum (Fig. 3D; Table 3). The activation overlapped with the superior part of the EBA but was absent in the inferoposterior EBA. Consistent with this observation, peak coordinates (local maxima) adjacent to those in the visual conditions were found in the left middle temporal gyrus, left superior temporal gyrus, and right angular gyrus (MNI coordinates indicated with asterisks in Table 4). The hand-sensitive activation was compared further between the two groups in the subsequent analyses.

Hand-sensitive activation regardless of visual experience

We evaluated the brain regions showing hand sensitivity, regardless of visual experience. This analysis used data from only the congenitally blind subjects, to exclude the effects of visual expe-

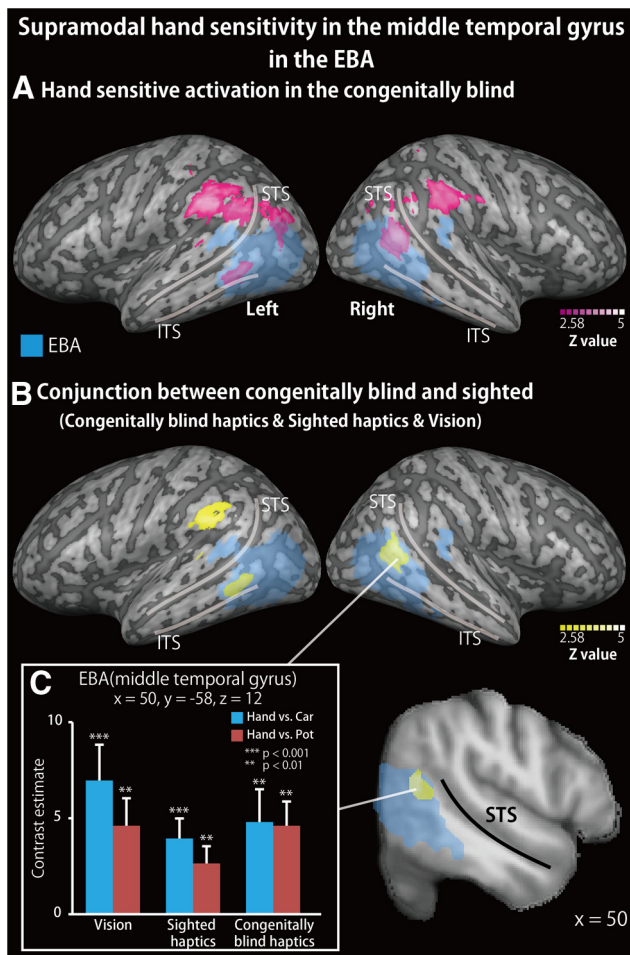


Figure 4. Supramodal hand-sensitive activation in the middle temporal gyrus of the EBA during the recognition of hand shapes. **A**, Hand-sensitive activation (response to hand stimuli relative to inanimate objects) observed during the haptic task in the congenitally blind group. The activation was thresholded at $p < 0.05$, corrected for multiple comparisons, with the height threshold set at $Z > 2.58$. Blue area represents the EBA as defined by an independent localizer task. STS, Superior temporal sulcus; ITS, inferior temporal sulcus. **B**, Conjunction analysis on hand-sensitive activation observed during the haptic task in the congenitally blind group, the haptic task in the sighted group, and the visual task in the sighted group (with the conjunction-null hypothesis). The same statistical threshold was applied as in **A**. See Table 5 for peak coordinates. **C**, Bar graphs represent response (contrast estimates) to hand compared with each of the other objects from the peak coordinate. Asterisks indicate the results of one-sample t tests. Data are presented as the mean \pm SEM of 18 congenitally blind and 28 sighted subjects.

rience. We initially examined hand-sensitive activation in the congenitally blind subjects. The whole-brain and ROI analyses confirmed significant hand-sensitive activation within the bilateral EBA of the congenitally blind subjects (Fig. 4A).

We then conducted a conjunction analysis of the hand-sensitive activation during the haptic condition in the sighted subjects, the visual condition in the sighted subjects, and the haptic condition in the congenitally blind subjects (with a conjunction-null hypothesis). The whole-brain analysis revealed significant hand-sensitive activation in the left supramarginal gyrus (Fig. 4B; Table 5). The subsequent ROI analysis revealed significant activation in the bilateral middle temporal gyrus and right angular gyrus within the EBA (Fig. 4B; Table 5). The peak coordinates within the EBA showed greater response to hands than to each class of inanimate objects, regardless of the sensory modality and the visual experience (p values < 0.05 , one-sample t tests; for the right EBA, Fig. 4C).

Cross-validation analysis

To confirm the patterns of hand response relative to each object class without the double-dipping problem, we conducted a split-half cross-validation analysis with EBA in each hemisphere as the ROI (Kriegeskorte et al., 2009). Table 6 shows the mean peak coordinates of haptic hand-sensitive activation. We localized a peak voxel in $>90\%$ of the subjects in each group (Table 6). In both groups, the mean coordinates were located in the middle temporal gyrus. The peak coordinates between the two groups were highly comparable; a statistical difference was found only in the x -coordinate in the right EBA ($t_{(41)} = 2.1, p < 0.05$, two-sample t test). Figure 5 shows the response (contrast estimate) to the perceived hand relative to each class of inanimate objects. We confirmed the greater response to the perceived hand relative to each of the other object classes in each sensory modality and in each group (p values < 0.05 , one-sample t tests). Collectively, these results confirmed that a greater response than that to each of the other object classes was present in the middle temporal gyrus within the EBA, regardless of the sensory modality and of visual experience.

Is the EBA activated by quantitative differences in motoric components across object categories?

Previous studies showed that quantitative differences in hand movement resulted in significant activity in the primary motor cortex (M1) (Dettmers et al., 1995; Sadato et al., 1997). If a quantitative difference in motoric components explains the hand-sensitive activation in the EBA, there should be correlated activity between the EBA and the M1. To examine this point, we conducted two analyses. First, we examined whether hand-sensitive activation was observed within the precentral gyrus in the haptic task; the hand-sensitive activity was negligible in each group (p values > 0.3 , cluster corrected over the precentral gyrus). Second, we conducted a simple regression analysis on all subjects (blind and sighted) with M1 activity as a covariate. To localize the M1, we evaluated the contrast of all object classes versus the baseline during the haptic task in each group, and then evaluated the conjunction between the two groups. We defined M1 activity as the parameter estimate at the peak coordinate of this analysis ($x = -34, y = -26, z = 52, Z$ value > 8.0). However, no significant activity was observed in the EBA. Collectively, these findings suggest that it is unlikely that hand-sensitive activity in the EBA can be simply explained by quantitative differences in hand movement.

Reduced hand selectivity in the blind group

To examine the effect of visual deprivation on hand sensitivity in the EBA, we compared the hand-sensitive activation in the sighted group with that in the blind group (including both congenitally and noncongenitally blind individuals). Whole-brain analysis revealed no significant area of activation. ROI analysis revealed regions showing activation differences in the left middle occipital gyrus (Fig. 6A; Table 7). Hand-sensitive activity (the contrast estimate of hand-related activation relative to toy cars and teapots) extracted from the peak coordinate correlated with neither the age at onset of total blindness (Fig. 6B) nor the relative performance accuracy (i.e., the performance accuracy for hands relative to the other objects; r values < 0.2).

Dependence of hand sensitivity on duration of early visual experience

We identified the brain regions in which the activity correlated with the length of early visual experience (Fig. 7; Table 8). As the

Table 5. Hand-sensitive activation, regardless of the sensory modality or visual experience^a

Spatial extent test/cluster size (mm ³)	<i>p</i> values	MNI coordinates			Z value	Hemisphere	Anatomical region
		<i>x</i>	<i>y</i>	<i>z</i>			
Conjunction of hand-sensitive activation among sighted haptics, sighted vision, and blind haptics (Fig. 4)							
816	<0.01*	50	−58	12	3.6	R	Middle temporal gyrus (EBA)
		52	−58	18	3.4	R	Angular gyrus (EBA)
480	<0.05*	−60	−54	0	3.6	L	Middle temporal gyrus (EBA)
1264	<0.05	−58	−40	32	4.5	L	Supramarginal gyrus

^aIn this analysis, we excluded the noncongenitally blind individuals. The activation was thresholded at *p* < 0.05, corrected for multiple comparisons, with the height threshold set at *Z* > 2.58. *x*, *y*, and *z* are stereotaxic coordinates (mm). R, Right; L, left.

*The search volume for activation was limited to the EBA in each hemisphere as defined by an independent visual localizer (ROI analysis).

Table 6. Mean coordinates localized by the split-half cross-validation analysis^a

	Congenitally blind				<i>n</i> (<i>M</i>)	Anatomical region	Sighted				<i>n</i> (<i>M</i>)	Anatomical region
	MNI coordinates			<i>z</i>			MNI coordinates			<i>z</i>		
	<i>x</i>	<i>y</i>	<i>z</i>				<i>x</i>	<i>y</i>	<i>z</i>			
Right EBA												
Mean	53.1	−56.2	4.9	17 (18)	Middle temporal gyrus	49.9	−58.9	3.5	26 (28)	Middle temporal gyrus		
SEM	1.3	2.2	2.3			0.9	1.1	1.4				
Left EBA												
Mean	−50.9	−61.4	5.1	18 (18)	Middle temporal gyrus	−48.6	−63.4	3.6	26 (28)	Middle temporal gyrus		
SEM	1.8	1.5	1.7			1.6	1.9	1.2				

^aMNI coordinates, mean peak coordinates of hand-sensitive activation within the EBA; *n*, number of subjects who showed hand-sensitive activation in at least one-half of the split data; *M*, total number of subjects in each group. See Figure 5 for response to each object category.

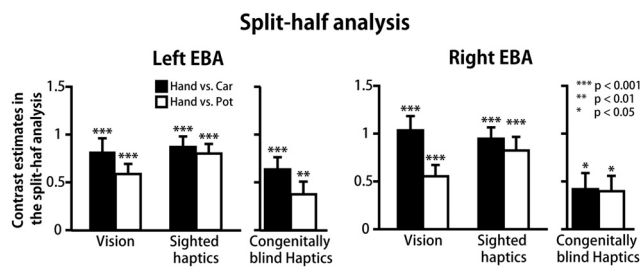


Figure 5. Response to recognized hand shapes in the cross-validation analysis. The split-half analysis on the haptic data of each group confirms that a greater response to hand (contrast estimate) than to each class of inanimate objects is present in the EBA without the double-dipping problem. Asterisks indicate the results of one-sample *t* tests. Mean peak coordinates were located in the middle temporal gyrus in both hemispheres, regardless of the group. See Table 6 for peak coordinates.

majority of the subjects were congenitally blind, we used nonparametric permutation tests (Nichols and Holmes, 2002). A simple regression analysis using the age at onset of total blindness revealed no significant region of activation in the whole-brain analysis. ROI analysis revealed significant activation in the right inferior temporal sulcus (Fig. 7A). We confirmed that the age at onset of total blindness significantly predicted hand-sensitive activity at the peak coordinate (Spearman’s $\rho = 0.46$, $p < 0.01$; Fig. 7B, top). The activity extracted from the peak coordinate was significantly correlated with the performance accuracy for hand shapes relative to the other objects (Spearman’s $\rho = 0.33$, $p < 0.05$, Fig. 7B, bottom). We confirmed that the same peak coordinate in the sighted group showed a greater response to hand shapes than to each of the other object classes in both the haptic and visual conditions (p values < 0.05, one-sample *t* tests on hand sensitivity). We observed no significant activation within the region where hand-sensitive activation was reduced in the blind group (Fig. 6).

Increased hand sensitivity in the blind group

The contrast of hand sensitivity in the blind group with that in the sighted group revealed regions of significant activation in the left

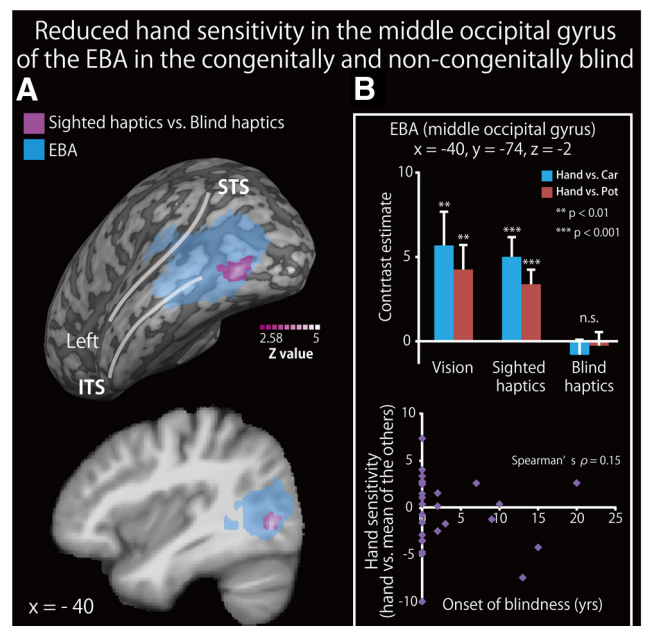


Figure 6. Reduced hand sensitivity in the middle occipital gyrus of the EBA in the blind subjects. **A**, Brain regions showing greater hand-sensitive activation in the sighted group than in the blind group (congenital and noncongenital) are shown in purple on a surface-rendered MRI (upper row) and a sagittal section (lower row) of an MRI averaged across the subjects. We used data from both the congenitally and noncongenitally blind subjects in this analysis. The activation was thresholded at $p < 0.05$, corrected for multiple comparisons over the EBA in each hemisphere, with the height threshold set at $Z > 2.58$. STS, Superior temporal sulcus; ITS, inferior temporal sulcus. See Table 7 for more information. **B**, Top, The contrast estimate (relative to each object class) extracted from the peak coordinate in the three conditions. Asterisks indicate the results of one-sample *t* tests. Bottom, Weak relationship between hand sensitivity and the age at onset of blindness. Data are presented as the mean \pm SEM of 28 blind and 28 sighted subjects.

angular gyrus (Fig. 8; Table 7). Neither the whole-brain nor the ROI analyses revealed significant activation in the EBA. The topographic effect of visual deprivation on hand sensitivity in the EBA is summarized in Figure 9.

Table 7. Group differences in hand-sensitive activation^a

Spatial extent test/cluster size (mm ³)	<i>p</i> values	MNI coordinates			Z value	Hemisphere	Anatomical region
		<i>x</i>	<i>y</i>	<i>z</i>			
Greater hand sensitivity in the sighted than in the blind (Fig. 6)							
496	<0.05*	−40	−74	−2	3.4	L	Middle occipital gyrus (EBA)
Greater hand sensitivity in the blind than in the sighted (Fig. 8)							
1800	<0.01	−54	−56	36	4.6	L	Angular gyrus

^aIn this analysis, we included both congenitally and noncongenitally blind individuals. The activation was thresholded at $p < 0.05$, corrected for multiple comparisons, with the height threshold set at $Z > 2.58$. *x*, *y*, and *z* are stereotaxic coordinates (mm). R, Right; L, left.

*The search volume for activation was limited to the EBA in each hemisphere as defined by an independent visual localizer (ROI analysis).

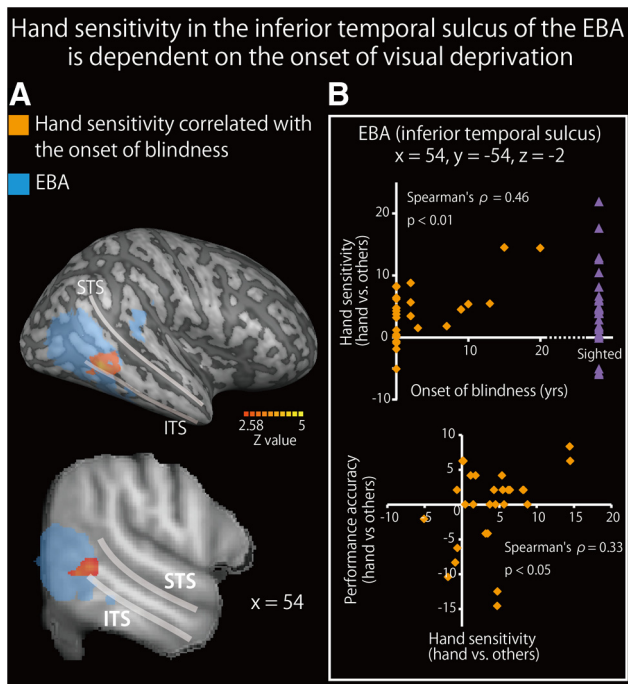


Figure 7. Hand sensitivity in the inferior temporal sulcus of the EBA is dependent on the age of visual loss (nonparametric analysis). **A**, Brain regions where hand sensitivity positively correlated with the age of visual loss are shown on a surface-rendered MRI (top row) and a sagittal section (bottom row) of an MRI averaged across the subjects. The activation was thresholded at $p < 0.05$, corrected for multiple comparisons in the EBA in each hemisphere, with the height threshold set at $Z > 2.58$. STS, Superior temporal sulcus; ITS, inferior temporal sulcus. See Table 8 for more information. **B**, The age at onset of blindness significantly predicted hand sensitivity (top) and hand sensitivity predicted performance accuracy (hands vs other objects) (bottom). Purple triangles represent the hand sensitivity of the sighted subjects. Data are presented as the mean \pm SEM of 28 blind and 28 sighted subjects.

Discussion

The present study demonstrated that the superior part of the EBA (i.e., the middle temporal gyrus and angular gyrus) showed hand-sensitive activation, regardless of sensory modality or visual experience. This result suggests that the functional sensitivity in the EBA can develop without visual experience. An increasing number of neuroimaging studies have shown that the functional organization of occipitotemporal regions is highly similar, regardless of visual experience, including the ventral visual pathway (Pietrini et al., 2004; Amedi et al., 2007; Mahon et al., 2009; Reich et al., 2011; Wolbers et al., 2011; Striem-Amit et al., 2012) and the dorsal visual pathway (Poirier et al., 2006; Ricciardi et al., 2007; Matteau et al., 2010; Renier et al., 2010; Collignon et al., 2011). Our results extend these findings by demonstrating that

the visual cortex responsible for the recognition of others' bodies can develop supramodally.

Our present findings were different from those recently reported by Striem-Amit et al. (2014) in two respects: (1) we demonstrated topographical effects of visual experience on the formation of the EBA, with only the superior part showing hand-sensitive activation without visual experience; and (2) we demonstrated that the EBA showed sensitivity to body parts supramodally when hands were recognized in an ecologically valid manner (i.e., by touch). Sensory-substitution device requires prolonged, intensive training (73 h on average) (Striem-Amit et al., 2014), which can induce plastic change in the functional organization of the occipitotemporal cortex. Thus, our result extends the previous finding by showing that a specific part of the EBA is critical for processing the recognition of hand shapes, when intensive training was not involved.

Supramodal hand-sensitive activation in the middle temporal gyrus in the EBA

We also observed vision-independent hand sensitivity in the supramarginal gyrus. Our result suggests that the superior part of the EBA and the supramarginal gyrus might constitute a cortical network for hand recognition, regardless of visual experience. The middle temporal gyrus and the inferior parietal lobule are considered critical nodes for action understanding (Rizzolatti et al., 2001; Iacoboni and Dapretto, 2006). Hand shapes can be considered as one such action class because they involve the contraction and relaxation of sets of muscles. The frontoparietal network is activated by the execution and recognition of actions in the sighted (Iacoboni and Dapretto, 2006) and the blind (Ricciardi et al., 2009). The middle temporal gyrus is anatomically connected to the frontoparietal network (Catani et al., 2005; Rilling et al., 2008). The EBA is also active during goal-directed movements of one's own body (Astafiev et al., 2004; Orlov et al., 2010). Oosterhof et al. (2010) used multivariate pattern analysis to show cross-modal response across the visual and motor modalities in the lateral occipitotemporal cortex, which possibly overlapped with the EBA. Therefore, kinesthetic feedback of self-actions might contribute to the formation of the supramodal representation of hand shapes in the superior part of the EBA and the supramarginal gyrus. This speculation is supported by a computer simulation model wherein nonvisual (such as kinesthetic and tactile) inputs are sufficient to construct spatial information about human body parts (Fuke et al., 2007). In sum, the superior part of the EBA might be "experience-expectant" for body perception: body information in nonvisual sensory modalities might drive the development of the visual cortex for the recognition of others' body parts.

Sensorimotor properties in the EBA indicate that this region plays a critical role in imitating others' actions (Jackson et al.,

Table 8. Hand-sensitive activity dependent on the age of onset of total blindness^a

Spatial extent test/cluster size (mm ³)	<i>p</i> values	MNI coordinates			Z value	Hemisphere	Anatomical region
		<i>x</i>	<i>y</i>	<i>z</i>			
Hand-sensitive activation correlated with the onset of blindness (nonparametric analysis, Fig. 7)	<0.05*	54	−54	−2	4.3	R	EBA (inferior temporal sulcus)

^aThe activation was thresholded at *p* < 0.05, corrected for multiple comparisons, with the height threshold set at *Z* > 2.58. *x*, *y*, and *z* are stereotaxic coordinates (mm). R, Right; L, left.

*The search volume for activation was limited to the EBA in each hemisphere as defined by an independent visual localizer (ROI analysis).

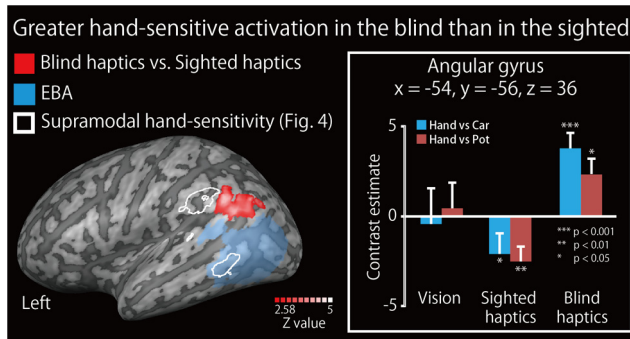


Figure 8. Increased hand sensitivity in the blind subjects. Brain regions revealing greater hand sensitivity (response to hands relative to inanimate objects) in the blind group than that in the sighted group are shown on a surface-rendered MRI (left). There was no overlap with the EBA. The activation was thresholded at *p* < 0.05, corrected for multiple comparisons over the whole brain, with the height threshold set at *Z* > 2.58. Bar graph on right represents the activity (i.e., contrast estimates for accurately identified hands relative to inanimate objects) extracted from the peak coordinate. Asterisks indicate the results of one-sample *t* tests. Data are presented as the mean ± SEM of 28 blind and 28 sighted subjects. Activity at the peak coordinate was not significantly correlated with the age at onset of blindness (Spearman's $\rho = 0.28$, *p* = 0.08). See Table 7 for more information.

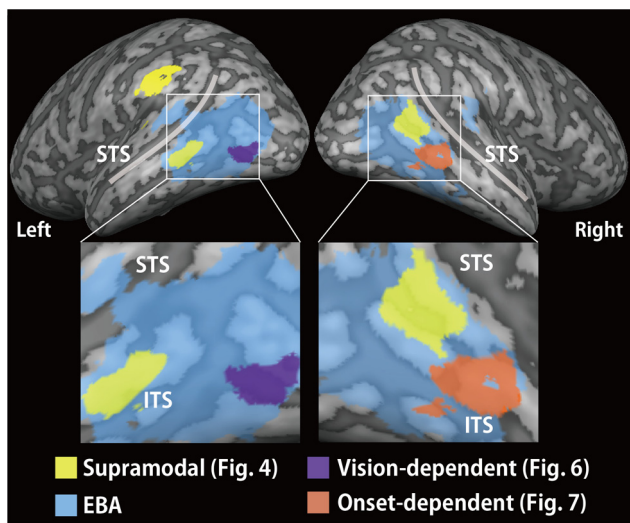


Figure 9. Summary of the present study. The supramodal subregion of the EBA is located in the middle temporal gyrus and angular gyrus, whereas the more inferior regions (the middle occipital gyrus and inferior temporal sulcus) were affected by visual experience. The activation patterns are superimposed on a surface-rendered T1-weighted high-resolution MRI averaged across the subjects. STS, Superior temporal sulcus; ITS, inferior temporal sulcus.

2006). Meltzoff (2005) proposed that imitation of others' actions is causally related to understanding others' mental state, that is, social cognition (the like-me hypothesis) (Meltzoff, 2005). If the EBA is critical not only for recognizing but also for imitating other's actions via haptics, this region might contribute to the development of social cognition even in the absence of vision.

Visual experience affects the development of hand preference in the inferior EBA

In contrast to the superior part, we found that visual experience affected the preference for hand stimuli in the inferior parts of the EBA (the inferior temporal sulcus and middle occipital gyrus). This suggests that the effect of early visual experience on the development of functional specialization can differ between the superior and inferior regions of the EBA. The inferior temporal sulcus showed hand-sensitive activation that was dependent on the duration of early visual experience (i.e., the age at which vision was lost). The duration of early visual experience also predicted individual differences in performance accuracy. However, the contribution of this region is less essential than that of the superior part of the EBA: in the blind group, even the least accurate performance (54%) was still well above the chance level (25%). Thus, this region might play a supplementary role in the recognition of hand shapes in blind individuals. This speculation is consistent with the notion that brain functional specialization can be influenced by postnatal factors because sensory experience is typically required for an innate mechanism to refine and develop toward a more mature form (Greenough et al., 1987; Lepänen and Nelson, 2009). Such postnatal factors might be reflected in the individual differences in behavioral performance in the hand-recognition task in the blind group (experience-dependent mechanism) (Leppänen and Nelson, 2009).

The middle occipital gyrus also showed reduced hand sensitivity as a result of visual deprivation. Unlike the inferior temporal sulcus, activity in this region was related neither to the length of visual experience nor to the task performance. This result suggests that the region does not play an essential role in the recognition of hand shapes in blind individuals. The reduced hand sensitivity in the middle occipital gyrus is consistent with the hypothesis that loss of visual input induces plastic changes in the functional organization of the occipital cortex (Sadato et al., 1996, 2002; Cohen et al., 1997; Burton et al., 2002a,b; Amedi et al., 2003, 2004). The critical period for the plastic changes in the primary visual cortex is ~15 years of age (Sadato et al., 2002). Here we found that there was a reduction of brain activity, even when the subject became blind at the age of 20 (Fig. 6B). Thus, it is possible that the critical period for plasticity in the middle occipital gyrus in the EBA is longer than that in the primary visual cortex. It remains an open question as to what roles the middle occipital gyrus in the blind individuals plays. For instance, the middle occipital gyrus is adjacent to the human homolog of area MT (hMT⁺), which is sensitive to motion stimuli (Tootell et al., 1995; Downing et al., 2007). In congenitally blind individuals, area hMT⁺ not only shows preference for moving stimuli perceived by touch (Ricciardi et al., 2007; Matteau et al., 2010), but also expands its sensitivity to include auditory moving stimuli (Poirier et al., 2006; Bedny et al., 2010). In the future, it will be important to localize hMT⁺ in the blind participants to examine how the preservation and expansion of spatial perceptual functions affect the formation of the EBA.

A point of interpretation should be noted in regard to the difference in response time between hands and inanimate objects (Fig. 2). Specifically, the subjects in both groups responded slightly later (0.8% of the response time for hand shapes) to hands than to one of the inanimate object categories (teapots) in the haptic task. However, in the haptic task, the subjects were asked to respond after a specified time period of exploration (7.5 s). Moreover, the response time of the sighted subjects showed the opposite pattern (i.e., a faster response for hands than the other categories of objects). Hence, it is unlikely that the differences in response time can explain the supramodal activation in the EBA.

In conclusion, the present study demonstrates that hand sensitivity in the EBA is variably affected by visual experience. Although the development of the inferior subregions was influenced by visual experience, the superior subregion, such as the middle temporal gyrus, developed its functional properties independent of visual experience. Our finding suggests that non-visual modalities can compensate for vision loss and develop the cortical network for hand recognition, even if its activity involves the visual cortex.

References

- Amedi A, Raz N, Pianka P, Malach R, Zohary E (2003) Early 'visual' cortex activation correlates with superior verbal memory performance in the blind. *Nat Neurosci* 6:758–766. [CrossRef Medline](#)
- Amedi A, Floel A, Knecht S, Zohary E, Cohen LG (2004) Transcranial magnetic stimulation of the occipital pole interferes with verbal processing in blind subjects. *Nat Neurosci* 7:1266–1270. [CrossRef Medline](#)
- Amedi A, Stern WM, Campodoni JA, Bermpohl F, Merabet L, Rotman S, Hemond C, Meijer P, Pascual-Leone A (2007) Shape conveyed by visual-to-auditory sensory substitution activates the lateral occipital complex. *Nat Neurosci* 10:687–689. [CrossRef Medline](#)
- Ashburner J (2007) A fast diffeomorphic image registration algorithm. *Neuroimage* 38:95–113. [CrossRef Medline](#)
- Ashburner J, Friston KJ (2005) Unified segmentation. *Neuroimage* 26:839–851. [CrossRef Medline](#)
- Astafiev SV, Stanley CM, Shulman GL, Corbetta M (2004) Extrastriate body area in human occipital cortex responds to the performance of motor actions. *Nat Neurosci* 7:542–548. [CrossRef Medline](#)
- Bedny M, Konkle T, Pelphrey K, Saxe R, Pascual-Leone A (2010) Sensitive period for a multimodal response in human visual motion area MT/MST. *Curr Biol* 20:1900–1906. [CrossRef Medline](#)
- Burton H, Snyder AZ, Conturo TE, Akbudak E, Ollinger JM, Raichle ME (2002a) Adaptive changes in early and late blind: a fMRI study of Braille reading. *J Neurophysiol* 87:589–607. [Medline](#)
- Burton H, Snyder AZ, Diamond JB, Raichle ME (2002b) Adaptive changes in early and late blind: a FMRI study of verb generation to heard nouns. *J Neurophysiol* 88:3359–3371. [CrossRef Medline](#)
- Catani M, Jones DK, ffytche DH (2005) Perisylvian language networks of the human brain. *Ann Neurol* 57:8–16. [CrossRef Medline](#)
- Cohen LG, Celnik P, Pascual-Leone A, Corwell B, Falz L, Dambrosia J, Honda M, Sadato N, Gerloff C, Catalá MD, Hallett M (1997) Functional relevance of cross-modal plasticity in blind humans. *Nature* 389:180–183. [CrossRef Medline](#)
- Collignon O, Vandewalle G, Voss P, Albouy G, Charbonneau G, Lassonde M, Lepore F (2011) Functional specialization for auditory-spatial processing in the occipital cortex of congenitally blind humans. *Proc Natl Acad Sci U S A* 108:4435–4440. [CrossRef Medline](#)
- Costantini M, Urgesi C, Galati G, Romani GL, Aglioti SM (2011) Haptic perception and body representation in lateral and medial occipito-temporal cortices. *Neuropsychologia* 49:821–829. [CrossRef Medline](#)
- Dettmers C, Fink GR, Lemon RN, Stephan KM, Passingham RE, Silbersweig D, Holmes A, Ridding MC, Brooks DJ, Frackowiak RS (1995) Relation between cerebral activity and force in the motor areas of the human brain. *J Neurophysiol* 74:802–815. [Medline](#)
- Downing PE, Jiang Y, Shuman M, Kanwisher N (2001) A cortical area selective for visual processing of the human body. *Science* 293:2470–2473. [CrossRef Medline](#)
- Downing PE, Wiggett AJ, Peelen MV (2007) Functional magnetic resonance imaging investigation of overlapping lateral occipitotemporal activations using multi-voxel pattern analysis. *J Neurosci* 27:226–233. [CrossRef Medline](#)
- Friston KJ, Jezzard P, Turner R (1994) Analysis of functional MRI time-series. *Hum Brain Mapp* 1:153–171. [CrossRef](#)
- Friston KJ, Holmes A, Poline JB, Price CJ, Frith CD (1996) Detecting activations in PET and fMRI: levels of inference and power. *Neuroimage* 4:223–235. [CrossRef Medline](#)
- Friston KJ, Glaser DE, Henson RN, Kiebel S, Phillips C, Ashburner J (2002) Classical and Bayesian inference in neuroimaging: applications. *Neuroimage* 16:484–512. [CrossRef Medline](#)
- Friston KJ, Penny WD, Glaser DE (2005) Conjunction revisited. *Neuroimage* 25:661–667. [CrossRef Medline](#)
- Friston KJ, Ashburner J, Kiebel SJ, Nichols TE, Penny WD (2007) *Statistical parametric mapping: the analysis of functional brain images*. London: Academic.
- Fuke S, Ogino M, Asada M (2007) Body image constructed from motor and tactile images with visual information. *Int J Hum Robot* 4:347–364. [CrossRef](#)
- Greenough WT, Black JE, Wallace CS (1987) Experience and brain development. *Child Dev* 58:539–559. [CrossRef Medline](#)
- Grol MJ, Majdandzic J, Stephan KE, Verhagen L, Dijkerman HC, Bekkering H, Verstraten FA, Toni I (2007) Parieto-frontal connectivity during visually guided grasping. *J Neurosci* 27:11877–11887. [CrossRef Medline](#)
- He C, Peelen MV, Han Z, Lin N, Caramazza A, Bi Y (2013) Selectivity for large nonmanipulable objects in scene-selective visual cortex does not require visual experience. *Neuroimage* 79:1–9. [CrossRef Medline](#)
- Holmes AP, Friston KJ (1998) Generalisability, random effects and population inference. *Neuroimage* 7:S754.
- Iacoboni M, Dapretto M (2006) The mirror neuron system and the consequences of its dysfunction. *Nat Rev Neurosci* 7:942–951. [CrossRef Medline](#)
- Jackson PL, Meltzoff AN, Decety J (2006) Neural circuits involved in imitation and perspective-taking. *Neuroimage* 31:429–439. [CrossRef Medline](#)
- Kitada R, Johnsrude IS, Kochiyama T, Lederman SJ (2009) Functional specialization and convergence in the occipito-temporal cortex supporting haptic and visual identification of human faces and body parts: an fMRI study. *J Cogn Neurosci* 21:2027–2045. [CrossRef Medline](#)
- Kitada R, Johnsrude IS, Kochiyama T, Lederman SJ (2010) Brain networks involved in haptic and visual identification of facial expressions of emotion: an fMRI study. *Neuroimage* 49:1677–1689. [CrossRef Medline](#)
- Kitada R, Okamoto Y, Sasaki AT, Kochiyama T, Miyahara M, Lederman SJ, Sadato N (2013) Early visual experience and the recognition of basic facial expressions: involvement of the middle temporal and inferior frontal gyri during haptic identification by the early blind. *Front Hum Neurosci* 7:7. [CrossRef Medline](#)
- Kriegeskorte N, Simmons WK, Bellgowan PS, Baker CI (2009) Circular analysis in systems neuroscience: the dangers of double dipping. *Nat Neurosci* 12:535–540. [CrossRef Medline](#)
- Lederman SJ, Klatzky RL (1987) Hand movements: a window into haptic object recognition. *Cogn Psychol* 19:342–368. [CrossRef Medline](#)
- Leppänen JM, Nelson CA (2009) Tuning the developing brain to social signals of emotions. *Nat Rev Neurosci* 10:37–47. [CrossRef Medline](#)
- Mahon BZ, Anzellotti S, Schwarzbach J, Zampini M, Caramazza A (2009) Category-specific organization in the human brain does not require visual experience. *Neuron* 63:397–405. [CrossRef Medline](#)
- Matteau I, Kupers R, Ricciardi E, Pietrini P, Ptito M (2010) Beyond visual, aural and haptic movement perception: hMT⁺ is activated by electrotactile motion stimulation of the tongue in sighted and in congenitally blind individuals. *Brain Res Bull* 82:264–270. [CrossRef Medline](#)
- Meltzoff AN (2005) Imitation and other minds: the 'like me' hypothesis. In: *Perspectives on imitation: from cognitive neuroscience to social science* (Hurley S, Chater N, eds), pp 55–77. Cambridge: Massachusetts Institute of Technology.
- Nichols TE, Holmes AP (2002) Nonparametric permutation tests for functional neuroimaging: a primer with examples. *Hum Brain Mapp* 15:1–25. [CrossRef Medline](#)
- Nichols T, Brett M, Andersson J, Wager T, Poline JB (2005) Valid conjunction inference with the minimum statistic. *Neuroimage* 25:653–660. [CrossRef Medline](#)
- Oldfield RC (1971) The assessment and analysis of handedness: the Edinburgh inventory. *Neuropsychologia* 9:97–113. [CrossRef Medline](#)

- Oosterhof NN, Wiggett AJ, Diedrichsen J, Tipper SP, Downing PE (2010) Surface-based information mapping reveals crossmodal vision-action representations in human parietal and occipitotemporal cortex. *J Neurophysiol* 104:1077–1089. [CrossRef Medline](#)
- Orlov T, Makin TR, Zohary E (2010) Topographic representation of the human body in the occipitotemporal cortex. *Neuron* 68:586–600. [CrossRef Medline](#)
- Peelen MV, Downing PE (2005a) Within-subject reproducibility of category-specific visual activation with functional MRI. *Hum Brain Mapp* 25:402–408. [CrossRef Medline](#)
- Peelen MV, Downing PE (2005b) Selectivity for the human body in the fusiform gyrus. *J Neurophysiol* 93:603–608. [CrossRef Medline](#)
- Peelen MV, Bracci S, Lu X, He C, Caramazza A, Bi Y (2013) Tool selectivity in left occipitotemporal cortex develops without vision. *J Cogn Neurosci* 25:1225–1234. [CrossRef Medline](#)
- Pietrini P, Furey ML, Ricciardi E, Gobbi MI, Wu WH, Cohen L, Guazzelli M, Haxby JV (2004) Beyond sensory images: object-based representation in the human ventral pathway. *Proc Natl Acad Sci U S A* 101:5658–5663. [CrossRef Medline](#)
- Poirier C, Collignon O, Scheiber C, Renier L, Vanlierde A, Tranduy D, Verraart C, De Volder AG (2006) Auditory motion perception activates visual motion areas in early blind subjects. *Neuroimage* 31:279–285. [CrossRef Medline](#)
- Reich L, Szwed M, Cohen L, Amedi A (2011) A ventral visual stream reading center independent of visual experience. *Curr Biol* 21:363–368. [CrossRef Medline](#)
- Renier LA, Anurova I, De Volder AG, Carlson S, VanMeter J, Rauschecker JP (2010) Preserved functional specialization for spatial processing in the middle occipital gyrus of the early blind. *Neuron* 68:138–148. [CrossRef Medline](#)
- Ricciardi E, Vanello N, Sani L, Gentili C, Scilingo EP, Landini L, Guazzelli M, Bichi A, Haxby JV, Pietrini P (2007) The effect of visual experience on the development of functional architecture in hMT⁺. *Cereb Cortex* 17:2933–2939. [CrossRef Medline](#)
- Ricciardi E, Bonino D, Sani L, Vecchi T, Guazzelli M, Haxby JV, Fadiga L, Pietrini P (2009) Do we really need vision? How blind people “see” the actions of others. *J Neurosci* 29:9719–9724. [CrossRef Medline](#)
- Rilling JK, Glasser MF, Preuss TM, Ma X, Zhao T, Hu X, Behrens TE (2008) The evolution of the arcuate fasciculus revealed with comparative DTI. *Nat Neurosci* 11:426–428. [CrossRef Medline](#)
- Rizzolatti G, Fogassi L, Gallese V (2001) Neurophysiological mechanisms underlying the understanding and imitation of action. *Nat Rev Neurosci* 2:661–670. [CrossRef Medline](#)
- Sadato N, Pascual-Leone A, Grafman J, Ibañez V, Deiber MP, Dold G, Hallett M (1996) Activation of the primary visual cortex by Braille reading in blind subjects. *Nature* 380:526–528. [CrossRef Medline](#)
- Sadato N, Ibañez V, Campbell G, Deiber MP, Le Bihan D, Hallett M (1997) Frequency-dependent changes of regional cerebral blood flow during finger movements: functional MRI compared to PET. *J Cereb Blood Flow Metab* 17:670–679. [CrossRef Medline](#)
- Sadato N, Okada T, Honda M, Yonekura Y (2002) Critical period for cross-modal plasticity in blind humans: a functional MRI study. *Neuroimage* 16:389–400. [CrossRef Medline](#)
- Shattuck DW, Mirza M, Adisetiyo V, Hojatkashani C, Salamon G, Narr KL, Poldrack RA, Bilder RM, Toga AW (2008) Construction of a 3D probabilistic atlas of human cortical structures. *Neuroimage* 39:1064–1080. [CrossRef Medline](#)
- Spiridon M, Fischl B, Kanwisher N (2006) Location and spatial profile of category-specific regions in human extrastriate cortex. *Hum Brain Mapp* 27:77–89. [CrossRef Medline](#)
- Striem-Amit E, Amedi A (2014) Visual cortex extrastriate body-selective area activation in congenitally blind people “seeing” by using sounds. *Curr Biol* 24:687–692. [CrossRef Medline](#)
- Striem-Amit E, Dakwar O, Reich L, Amedi A (2012) The large-scale organization of “visual” streams emerges without visual experience. *Cereb Cortex* 22:1698–1709. [CrossRef Medline](#)
- Tootell RB, Reppas JB, Kwong KK, Malach R, Born RT, Brady TJ, Rosen BR, Belliveau JW (1995) Functional analysis of human MT and related visual cortical areas using magnetic resonance imaging. *J Neurosci* 15:3215–3230. [Medline](#)
- Wager TD, Nichols TE (2003) Optimization of experimental design in fMRI: a general framework using a genetic algorithm. *Neuroimage* 18:293–309. [CrossRef Medline](#)
- Weiner KS, Grill-Spector K (2011) Not one extrastriate body area: using anatomical landmarks, hMT⁺, and visual field maps to parcellate limb-selective activations in human lateral occipitotemporal cortex. *Neuroimage* 56:2183–2199. [CrossRef Medline](#)
- Wolbers T, Klatzky RL, Loomis JM, Wutte MG, Giudice NA (2011) Modality-independent coding of spatial layout in the human brain. *Curr Biol* 21:984–989. [CrossRef Medline](#)
- Worsley KJ, Friston KJ (1995) Analysis of fMRI time-series revisited—again. *Neuroimage* 2:173–181. [CrossRef Medline](#)